



HAL
open science

Indirect excitation of Er³⁺ ions in silicon nitride films prepared by reactive evaporation

E. Steveler, H. Rinnert, X. Devaux, M. Dossot, M. Vergnat

► **To cite this version:**

E. Steveler, H. Rinnert, X. Devaux, M. Dossot, M. Vergnat. Indirect excitation of Er³⁺ ions in silicon nitride films prepared by reactive evaporation. *Applied Physics Letters*, 2010, 97 (22), pp.221902. 10.1063/1.3521279 . hal-02164303

HAL Id: hal-02164303

<https://hal.science/hal-02164303>

Submitted on 24 Jun 2019

HAL is a multi-disciplinary open access archive for the deposit and dissemination of scientific research documents, whether they are published or not. The documents may come from teaching and research institutions in France or abroad, or from public or private research centers.

L'archive ouverte pluridisciplinaire **HAL**, est destinée au dépôt et à la diffusion de documents scientifiques de niveau recherche, publiés ou non, émanant des établissements d'enseignement et de recherche français ou étrangers, des laboratoires publics ou privés.

Indirect excitation of Er³⁺ ions in silicon nitride films prepared by reactive evaporation

E. Steveler,¹ H. Rinnert,^{1,a)} X. Devaux,¹ M. Dossot,² and M. Vergnat¹

¹*Institut Jean Lamour, UPVM, CNRS, Nancy-University, Boulevard des Aiguillettes, B.P. 239, 54506 Vandœuvre-lès-Nancy Cedex, France*

²*Laboratoire de Chimie Physique et Microbiologie pour l'Environnement, UMR 7564 CNRS—Nancy-University, 405, rue de Vandœuvre, 54600 Villers-lès-Nancy, France*

(Received 22 July 2010; accepted 4 November 2010; published online 29 November 2010)

Er-doped silicon nitride films were obtained by reactive evaporation of silicon under a flow of nitrogen ions and were annealed at temperatures up to 1300 °C. Samples were studied by infrared absorption and Raman spectrometries and by transmission electron microscopy. The 1.54 μm Er-related photoluminescence (PL) was studied in relation with the structure with pump excitation at 488 and 325 nm. Steady-state PL, PL excitation spectroscopy, and time-resolved PL were performed. The results demonstrate that Er³⁺ ions are indirectly excited both via silicon nanocrystals and via localized states in the silicon nitride matrix. © 2010 American Institute of Physics. [doi:10.1063/1.3521279]

Er-doped silicon-based materials have attracted much attention in the scientific community because of their potential use for optoelectronics.¹ Indeed, Er³⁺ ions can emit sharp luminescence at 1.54 μm, which is the commonly used wavelength for optical communications. The Er sensitization has been widely studied in Si rich SiO₂ layers. In silica containing silicon nanocrystals (Si-nc), the Er-related photoluminescence is strongly improved due to a strong energy transfer from Si-nc to Er³⁺ ions.^{2–4} The Er³⁺ ions can then be indirectly excited by Si-nc which have an absorption cross section several orders of magnitude higher than that of direct Er excitation. While SiN_x is a particularly interesting host matrix for electrically pumped light-emitting devices, the Er excitation mechanism in silicon nitride films is still not clear. Similarly to the SiO_x based samples, the sensitization of Er³⁺ ions by Si nanoparticles has been reported in SiN_x samples prepared by plasma enhanced chemical vapour deposition (PECVD)⁵ or by magnetron sputtering.⁶ However, some works have also demonstrated that indirect excitation of Er³⁺ ions could occur via electronic states localized in the SiN_x band tail states.^{7,8}

In this letter, we study the Er-related PL at 1.54 μm in Er-doped silicon nitride thin films prepared by an ion-beam-assisted evaporation technique. The evolutions of the structure and of the PL properties with the annealing treatments are studied. It is demonstrated that the Er excitation is indirect and that Si-nc is able to improve the PL intensity. It is also shown that another indirect excitation path presumably exists in the amorphous SiN_x matrix.

Silicon was evaporated from an electron beam gun with a deposition rate equal to 0.1 nm/s. The 200 nm thick films were deposited on silicon substrates maintained at 100 °C. The nitrogen ions were provided by an electron cyclotron resonance microwave plasma source. The nitrogen flow was regulated by maintaining the total pressure in the evaporation chamber at 2 × 10⁻⁵ Torr. The Er doping was performed from an effusion cell. Rutherford backscattering spectrometry was used to analyze the chemical content of the film.

The Si, N, O, and Er atomic concentrations are equal to 47%, 48%, 5%, and 0.3%, respectively. The oxygen content is due to the low density of the layer and to exposure to the air. This concentration corresponds to a 12 at. % Si excess compared to the Si₃N₄ equilibrium stoichiometry.

The Fourier transform infrared (FTIR) experiments were carried out with a spectrometer with a resolution of 2 cm⁻¹. Raman measurements were carried out with a multichannel spectrometer equipped with a 1800 grooves mm⁻¹ grating. The samples were excited by the 514 nm line from an argon laser. Transmission electron microscopy was performed with a 200 keV microscope. For the steady-state PL experiments, the samples were excited by a 30 mW He–Cd laser using the 325 nm line or by a 60 mW laser diode emitting at 488 nm. For the PL excitation (PLE) experiments, the samples were excited by an optical parametric oscillator laser. The PL signal was measured by a photomultiplier tube cooled at 190 K. For the time-resolved PL experiments, the samples were pumped by the 355 nm line of a frequency-tripled YAG:Nd laser. The laser pulse frequency, energy, and duration were typically equal to 10 Hz, 50 μJ, and 20 ns, respectively. The time response of the detection system was better than 1 μs.

Figure 1(a) shows the FTIR spectra of the films for as-deposited sample and samples annealed at 1000 and 1100 °C. The spectrum shows a very intense band at around 850 cm⁻¹, characteristic of the asymmetric stretching vibration of the Si–N bonds.⁹ The spectra are not significantly modified for annealing temperatures lower than 1000 °C since only a 6 cm⁻¹ shift occurs to higher wavenumbers. For higher annealing temperature, the peaks shift again a few cm⁻¹ and a shoulder appears at high wavenumbers, demonstrating a modification of the Si–N bonds, which could be correlated to the precipitation of Si-nc.¹⁰

The Raman spectrum of bulk crystalline silicon exhibits a very thin band at 520 cm⁻¹ corresponding to the transverse optical mode. A weak contribution at around 300 cm⁻¹ is due to longitudinal acoustic mode. In amorphous silicon, the Raman spectrum presents two broad bands at 150 and at 480 cm⁻¹. Figure 1(b) shows Raman shifts for the different annealing temperatures. The as-deposited sample shows the

^{a)}Electronic mail: herve.rinnert@ijl.nancy-universite.fr.

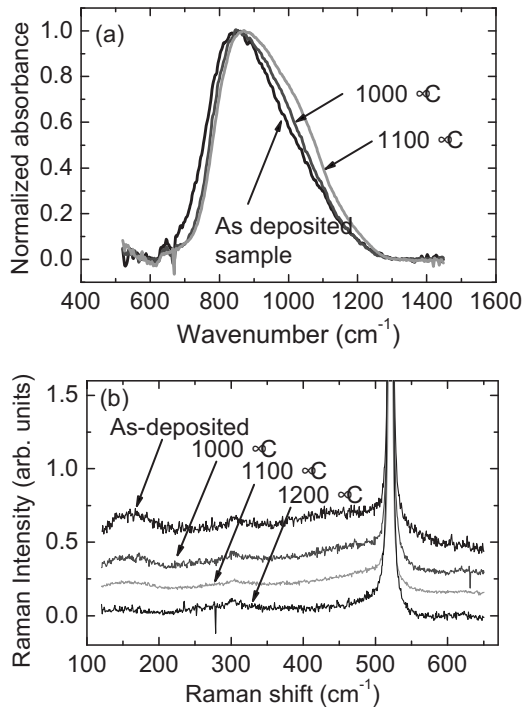


FIG. 1. (a) Infrared absorption spectra and (b) Raman shift for different annealing temperatures.

characteristic bands of pure amorphous silicon. This suggests that a part of the Si excess form amorphous Si domains in the SiN_x matrix. For samples annealed at temperatures higher than 700 °C, these amorphous contributions decrease with a more pronounced decrease for the samples annealed at 1100 °C. For higher annealing temperatures, the amorphous peaks disappear, which corresponds to the formation of crystalline domains.¹¹ The Raman peak due to the crystalline domains of the layer is not visible because of the strong response of the substrate.

Figure 2 shows micrographs for samples annealed at 700 and 1100 °C, respectively. While the micrograph is characteristic of amorphous sample for sample annealed at 700 °C, the micrograph demonstrates the existence of Si-nc for the sample annealed at 1100 °C. The size distribution is wide and the average Si-nc size is equal to a few nanometers. The samples remain amorphous until an annealing temperature equal to 1000 °C and the amorphous silicon clusters crystallize for higher annealing temperatures. With a Si excess equal to 12 at. %, a Si-nc mean size equal to 3.5 nm and a density of silicon and silicon nitride equal to 2.32 and 3.2, respectively, the density of Si-nc is estimated to 9.10¹⁷ cm⁻³.

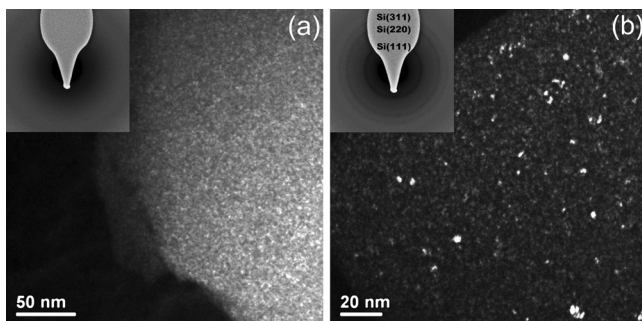


FIG. 2. Dark field views of samples annealed at (a) 700 °C (a) and at (b) 1100 °C.

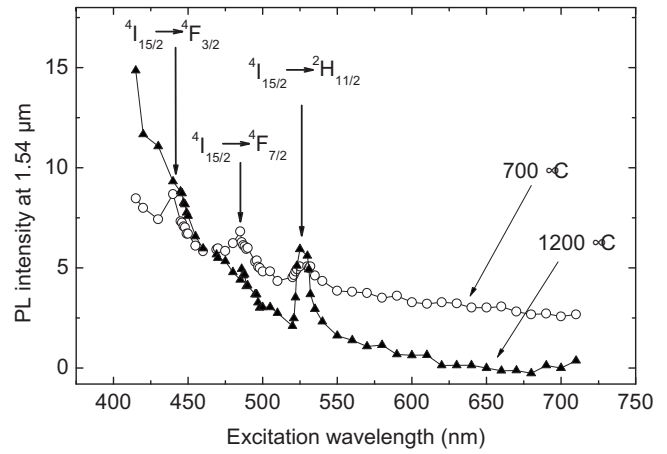


FIG. 3. Photoluminescence excitation spectra at 1.54 μm for samples annealed at 700 and 1200 °C.

This value probably overestimates the number of crystals because it assumes that all the Si excess contribute to form Si-nc.

Photoluminescence excitation spectra at 1.54 μm are presented in Fig. 3 for samples annealed at 700 and 1200 °C. No PL signal is obtained for the as-deposited sample. These results clearly show the characteristic direct excitation of Er³⁺ ions at 440, 486, and 528 nm, corresponding to the absorption from the ground state to the excited states ⁴F_{3/2}, ⁴F_{7/2}, and ²H_{11/2}, respectively. For both samples, the PLE spectra show nonresonant excitation of Er³⁺ ions, demonstrating an indirect excitation of the ions. This indirect process is a decreasing function of the excitation wavelength, with a more pronounced increase for the sample annealed at high temperature.

The dependence of the PL spectra with annealing temperatures is shown in Figs. 4(a) and 4(b) for excitation wavelengths equal to 325 and 488 nm, respectively. The same photon flux was used in both cases. Samples have been measured on the same setup, with the same experimental conditions. Hence PL intensities can be compared. Whatever the excitation wavelength, no Er-related PL is measured in the as-deposited samples. An annealing at 500 °C induces in the optical activation of the Er³⁺ ions and the PL intensity at

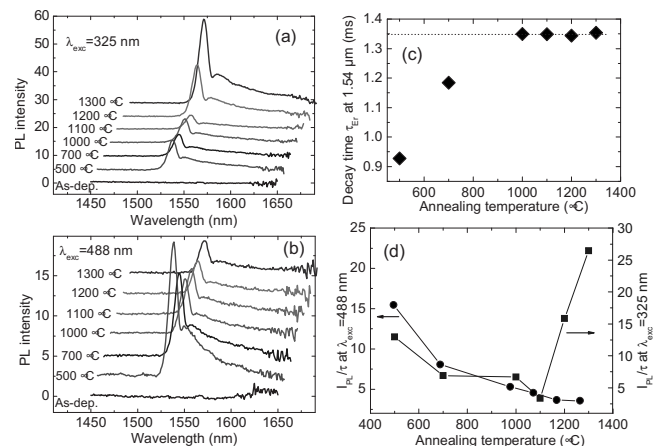


FIG. 4. Influence of the annealing temperatures on the PL spectra for excitation at (a) 325 nm and (b) 488 nm. (c) Decay time for the different annealing temperatures. (d) Dependence of the I_{PL} / τ_{ER} ratio with the annealing temperature for excitation wavelengths equal to 325 nm (■) or 488 nm (●).

1.54 μm is very similar for both excitation wavelengths. However, the dependence of the PL for higher annealing temperatures is strongly different. For the 325 nm excitation, the PL intensity is almost constant up to 1000 °C and strongly increases for higher annealing temperatures, while, under the 488 nm excitation, the PL intensity is a continuously decreasing function of the annealing temperature.

The 488 nm wavelength is known to be resonant with the $^4I_{15/2} \rightarrow ^4F_{7/2}$ transition of Er^{3+} ions. As shown by the PLE experiments, Er^{3+} ions are not dominantly excited through the direct absorption process at this wavelength. The PL intensity decrease with annealing treatments could be explained by an increasing number of nonradiative decay channels, like the formation of Er clusters. However, the PL intensity does not follow the same evolution under the 325 nm excitation. Moreover, the PL decay time τ_{Er} , shown in Fig. 4(c), is an increasing function of the annealing temperature, which is not in agreement with the appearance of nonradiative recombination. On the contrary, the increasing decay time values suggest that some nonradiative defects have been passivated by the annealing treatment. The dependence of the PL intensity with the annealing temperature suggests that the indirect excitation process occurring at 488 nm is strongly reduced with annealing treatments.

Si-ncs are known to be efficient sensitizers for Er^{3+} ions. Modeling using coupled rate equations is commonly reported in the literature to take into account of the excitation of Er^{3+} ions with sensitizers.^{12,13} In the low pump flux regime, the 1.54 μm PL intensity can be given by

$$I_{\text{PL}} = \frac{\sigma_{\text{Er}} \Phi \tau_{\text{Er}}}{1 + \sigma_{\text{Er}} \Phi \tau_{\text{Er}}} I_{\text{max}}, \quad (1)$$

where σ_{Er} , τ_{Er} , and Φ are the effective excitation cross section of Er^{3+} ions, the PL decay time, and the pump photon flux, respectively. I_{max} is proportional to the ratio of the total number of optically activated Er^{3+} ions divided by the radiative decay time. Figure 4(d) shows the $I_{\text{PL}}/\tau_{\text{Er}}$ ratio measured for the 325 and 488 nm excitations for the different samples studied. This ratio is a continuously decreasing function of the annealing temperature for the 488 nm excitation wavelength. Interestingly, the same behavior is obtained for the 325 nm excitation but only for annealing temperatures up to 1000 °C. For higher annealing temperatures, the ratio $I_{\text{PL}}/\tau_{\text{Er}}$ strongly increases. These results suggest that two different indirect excitation processes occur, depending on the annealing temperature and on the excitation wavelength. As the trend change in the dependence of $I_{\text{PL}}/\tau_{\text{Er}}$ with the annealing temperature around 1100 °C occurs simultaneously with the appearance of Si-nc, the obtained PL enhancement with the 325 nm excitation could be due to an energy transfer process from Si-nc to Er^{3+} ions. However, the behavior is different for the 488 nm excitation, while Si-nc should also contribute to the energy transfer with this excitation energy. By measuring the excitation power dependence of the PL intensity at 488 nm, the excitation cross-section has been measured for the sample annealed at 1200 °C. It is equal to $2 \times 10^{-17} \text{ cm}^2$, which is around one order of magnitude lower than that generally obtained for Er-doped Si rich SiO_2 layers.^{12,14} This low value could be explained by the weak number of Si-nc that can couple with Er^{3+} ions. The different

evolutions obtained with both excitation wavelengths can be explained by the fact that the absorption cross section of Si-nc is a decreasing function of the wavelength. More precisely, Izeddin *et al.*¹⁴ have shown that the PL excitation cross-section of Si-nc is five times higher at 355 nm than at 488 nm. The value at 325 nm can then be estimated to be around one order of magnitude higher than at 488 nm. This result could then explain the different trends presented in Fig. 4(d). For samples annealed below 1100 °C, and for an excitation at 488 nm, the role of Si-nc on the Er-related PL is negligible compared to the matrix-mediated Er excitation cross section. For the excitation at 488 nm and for the excitation at 325 nm in case of samples annealed below 1100 °C, Er^{3+} ions are probably excited via disorder-induced localized states in the SiN_x band tails, as already mentioned in the literature.⁸ As previously shown in similar SiN_x layers, the optical gap is an increasing function of the annealing temperature, which is explained by a decrease of the density of states in the SiN_x gap.¹⁵ The annealing-induced decrease of the electronic state density in the gap could then involve in the decrease of sensitization of Er^{3+} ions via localized states in the gap.

In conclusion, Er related PL at 1.54 μm was studied in Si-rich silicon nitride films. It is shown that an indirect energy transfer process, dependent on the structure of the films, is involved in the excitation of Er^{3+} ions. For low annealing temperatures, samples are amorphous and the electronic states that coupled with Er^{3+} ions are probably due to disorder-induced localized states in the SiN_x bandgap. For annealing temperatures greater than 1100 °C, Si-nc could play a major role in the energy transfer process for low excitation wavelength.

¹A. Polman, *J. Appl. Phys.* **82**, 1 (1997).

²G. Franzo, D. Pacifici, V. Vinciguerra, F. Priolo, and F. Iacona, *Appl. Phys. Lett.* **76**, 2167 (2000).

³M. Fujii, M. Yoshida, Y. Kansawa, S. Hayashi, and K. Yamamoto, *Appl. Phys. Lett.* **71**, 1198 (1997).

⁴H. Rinnert, G. Wora Adeola, and M. Vergnat, *J. Appl. Phys.* **105**, 036101 (2009).

⁵N. M. Park, T. Y. Kim, S. H. Kim, G. Y. Sung, K. S. Cho, J. H. Shin, B. H. Kim, S. J. Park, J. K. Lee, and M. Nastasi, *Thin Solid Films* **475**, 231 (2005).

⁶L. Dal Negro, R. Li, J. Warga, and S. N. Basu, *Appl. Phys. Lett.* **92**, 181105 (2008).

⁷Q. Zhao, H. Yan, M. Kumeda, and T. Shimizu, *Appl. Surf. Sci.* **227**, 306 (2004).

⁸S. Yerci, R. Li, S. O. Kucheyev, T. van Burren, S. N. Basu, and L. Dal Negro, *Appl. Phys. Lett.* **95**, 031107 (2009).

⁹D. V. Tsu, G. Lucovsky, and M. J. Mantini, *Phys. Rev. B* **33**, 7069 (1986).

¹⁰G. Scardera, T. Puzzer, G. Conibeer, and M. A. Green, *J. Appl. Phys.* **104**, 104310 (2008).

¹¹M. Molinari, H. Rinnert, M. Vergnat, and P. Weisbecker, *Mater. Sci. Eng., B* **101**, 186 (2003).

¹²D. Pacifici, G. Franzo, F. Priolo, F. Iacona, and L. Dal Negro, *Phys. Rev. B* **67**, 245301 (2003).

¹³B. Garrido, C. Garcia, S. Y. Seo, P. Pellegrino, D. Navarro-Urrios, N. Dalosso, L. Pavesi, F. Gourbilleau, and R. Rizk, *Phys. Rev. B* **76**, 245308 (2007).

¹⁴I. Izeddin, D. Timmerman, T. Gregorkiewicz, A. S. Moskelenko, A. A. Prokoviev, I. N. Yassievich, and M. Fujii, *Phys. Rev. B* **78**, 035327 (2008).

¹⁵M. Molinari, H. Rinnert, and M. Vergnat, *Appl. Phys. Lett.* **77**, 3499 (2000).